Total reflection and surface scattering of soft X-rays on the Si-SiO_2 system and hexagonal BN crystal

1995 J. Phys.: Condens. Matter 7 2731

(http://iopscience.iop.org/0953-8984/7/14/012)

J. Phys.: Condens. Matter 7 (1995) 2731–2744. Printed in the UK

Total reflection and surface scattering of soft x-rays on the Si–SiO_2 system and hexagonal BN crystal

E Filatova†, A Stepanov†, C Blessing‡, J Friedrich‡, R Barchewitz§‖, J-M André§‖, F Le Guern§‖, S Bac§‖ and P Troussel‖¶

† Institute of Physics, St Petersburg University, St Petersburg 198904, Russia
‡ Institut für Experimentalphysik, Universität Hamburg, D-2000 Hamburg 50, Germany
§ Laboratoire de Chimie Physique-Matière et Rayonnement, Université Pierre et Marie Curie, Unité associée au CNRS 176, 75231 Paris Cédex 05, France
‖ Laboratoire pour l'Utilisation du Rayonnement Electromagnétique, Université Paris Sud, 91405 Orsay, France
¶ Commissariat à l'Energie Atomique, Centre d'Etudes de Limeil-Valenton, 94195 Villeneuve St Georges, France

Received 14 October 1994, in final form 3 January 1995

Abstract. Reflection spectra for different grazing angles and reflectivity angular dependences of the Si–SiO_2 system with different dioxide thicknesses have been measured in the energy range 40–850 eV, including the Si $L_{2,3}$ and O K absorption edges. The angular dependences have been used for the dielectric constant determination. By turning a BN hexagonal crystal and using s-polarized radiation a strong reflectivity dependence on the crystal orientation has been detected. Indicatrices of the surface roughness scattering have been recorded for the BN_{hex} crystal surface. The statistical properties of the roughness have been investigated by means of perturbation theory. These measurements were obtained using synchrotron radiation, and the interest in the specific properties of this radiation for such measurements is emphasized.

1. Introduction

There is increasing interest in soft-x-ray reflection spectroscopy as a surface- and interface-sensitive method which is now well recognized as a very efficient non-destructive method of material diagnostics (Martens and Rabe 1980, Greaves *et al* 1990). However, although a few x-ray reflection spectroscopy studies (André *et al* 1982) and surface diffuse scattering measurements (Hogrefe and Kunz 1987) using synchrotron radiation have been reported, most x-ray reflectometry investigations make use of standard x-ray tubes. Unfortunately, the utilization of laboratory sources of radiation restricts significantly the possibilities of this method. Synchrotron radiation characterized by high intensity, broad spectral range, small divergence and linear polarization can help to realize the capabilities of x-ray reflectometry to the greatest extent. The realization of the possibilities of x-ray reflection spectroscopy and reflectometry is demonstrated in this report. We emphasize the interest in the wide spectral domain and the low beam divergence available with synchrotron radiation through the study of the Si–SiO_2 layer system and the interest in linear polarization through the study of the anisotropic boron nitride hexagonal crystal. We also utilize the low beam divergence and the high flux to perform the diffuse scattering measurements.

The paper is organized as follows: section 2 summarizes the physical models used to analyse the experimental data, section 3 gives the experimental procedures, and the results are presented and discussed in section 4.

0953-8984/95/142731+14$19.50

2. Physical models

In the x-ray range the dielectric constant ε is conveniently expressed in the following way:

$$\varepsilon = 1 - \delta + i\beta. \tag{1}$$

In the framework of the Fresnel model on the assumption of a perfectly smooth flat surface-limiting vacuum and a homogeneous substance of dielectric constant ε, the reflection amplitude r in the s configuration (the electric field perpendicular to the plane of incidence) can be written in the following way:

$$r_s = \frac{\sin\theta - \sqrt{\varepsilon - \cos^2\theta}}{\sin\theta + \sqrt{\varepsilon - \cos^2\theta}} \tag{2}$$

where θ is the glancing angle measured with respect to the surface.

Experimentally one measures the reflectivity $R = |r|^2$. The behaviour of the reflectivity versus the glancing angle has been discussed in detail elsewhere (André *et al* 1984). This Fresnel model can be extended to a stratified medium, i.e. to a medium whose dielectric constant varies only with the depth (Parratt 1954). Thus for a single layer (indicated by subscript l) of thickness d and dielectric constant ε_l located between the incident medium (vacuum indicated by subscript v) and an unbounded medium (semi-infinite substrate indicated by subscript s) the reflection coefficient is written

$$r = \frac{r_{vl} + r_{ls}\exp[2id(\omega/c)\sqrt{\varepsilon_l - \cos^2\theta}]}{1 + r_{vl}r_{ls}\exp[2id(\omega/c)\sqrt{\varepsilon_l - \cos^2\theta}]} \tag{3}$$

where r_{ij} is the Fresnel coefficient at the interface between i and j, and ω/c is the wavenumber in vacuum. This kind of formula has been used to analyse the Si–SiO_2 layer system.

Of special interest is the investigation of the near-edge x-ray absorption fine structure (NEXAFS) which reflects the energy distribution of the conduction band electron states and is very sensitive to the chemical composition of the substance. It is interesting to evaluate in this connection the thickness of the layers determining the reflection in the x-ray region, or the radiation penetration depth. It depends upon the incidence angle, of course. Considering an exponential decrease in intensity we have the following evaluation of its characteristic scale:

$$\frac{1}{D} = 2\frac{\omega}{c}\,\mathrm{Im}\left(\sqrt{\varepsilon - \cos^2\theta}\right). \tag{4}$$

In the soft-x-ray region, typical values of D are about 1–50 nm. In fact, the penetration depth is the available depth of probing. So, the soft-x-ray reflectometry method has a unique capability in investigating the surface on a nanometric scale. From the reflectivity measurements, it is possible to deduce, at least on a relative scale, the spectral dependence of the absorption coefficient by means of a Kramers–Kronig analysis.

So far it has been assumed that the reflecting surfaces are flat surfaces, but all real surfaces have roughness. To describe the x-ray reflection and scattering from rough surfaces, many theoretical approaches have been developed, but all purely analytical models are perturbation theories assuming that the mean roughness height is less than the wavelength of the radiation. Unfortunately this condition is rarely fulfilled in the x-ray region.

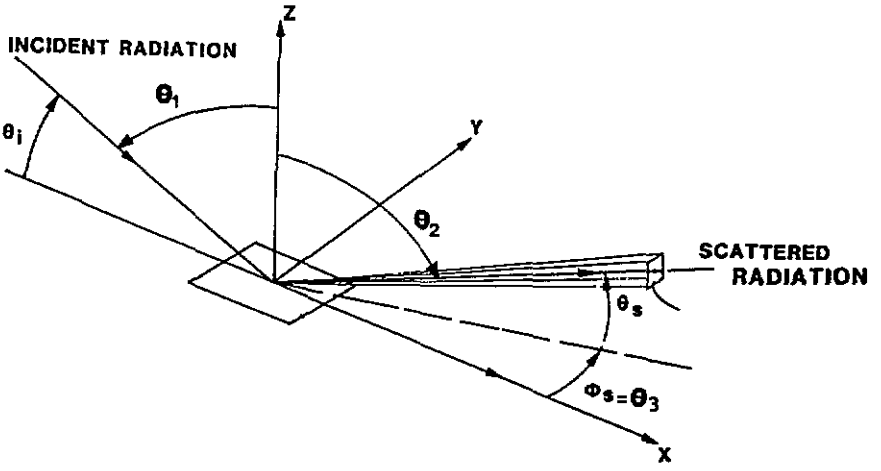

Figure 1. Geometry of the surface scattering.

Traditionally the boundary between the substance and the vacuum is described by the equation $z = \zeta(\rho)$, where ζ can be considered as a random function which determines the statistical characteristics of the boundary. The vector ρ lies in the (x, y) plane. The statistical properties of the surface are usually described by an autocorrelation function (ACF) $\chi(\rho - \rho') = \langle \zeta(\rho)\zeta(\rho') \rangle$. The quantity $\sigma = \sqrt{\chi(0)}$ is the mean roughness height corresponding to roughness characterized by the ACF $\chi(\rho)$. It has been shown that it is sometimes necessary to use several ACFs to describe the roughness statistics of a given surface (Noll and Glenn 1982); each ACF is relative to a scale of correlation called the correlation length. In the case of isotropic roughness, the ACF depends only on the quantity $\rho = |\rho|$. The characteristic scale of variation in $\chi(\rho)$ is called the correlation radius. Most of the surfaces present an isotropic roughness and an ACF corresponding to a short correlation length, which is well described by a Gaussian function; in these conditions the ACF is written

$$G(\rho) = \sigma^2 \exp\left(-\frac{\rho^2}{T^2}\right) \tag{5}$$

where T is the autocorrelation radius. Let us recall the basic results of the perturbation theories modelling the diffuse scattering from surface roughness. The scattered intensity $dI_s/d\Omega$ per unit solid angle is given by

$$\frac{dI_s}{d\Omega} = \frac{1}{\pi^4}\left(\frac{\omega}{c}\right)^4 \cos\theta_1 \cos^2\theta_2 W Q(\theta_1, \theta_2, \theta_3, \varepsilon) \tag{6}$$

where W is the power spectral density function (PSDF) of the surface roughness which is obtained as the Fourier transform of the ACF, and Q is the polarization-dependent function of the angles and of the complex dielectric constant ε of the medium considered as a homogeneous material. For scattering in the plane of incidence ($\theta_3 = 0$), in the s configuration without change in polarization, Q is given by (Maradudin and Mills 1975)

$$Q = \frac{|\varepsilon - 1|^2}{|\cos\theta_2 + \sqrt{\varepsilon - \sin^2\theta_2}|^2 |\cos\theta_1 + \sqrt{\varepsilon - \sin^2\theta_1}|^2}. \tag{7}$$

The geometry is given in figure 1. Similar or slightly different models can be found in the literature (Elson 1984) but all of them suffer from the limitations inherent in their perturbative nature.

The attenuation of the specular reflection is generally given by the so-called Debye–Waller formula which is written in terms of reflectivity as follows:

$$R_R = R_F \exp\left[-\left(2\frac{\omega}{c}\sin\theta\sigma\right)^2\right] \tag{8}$$

where σ is the mean roughness height, R_R the reflectivity of the rough surface and R_F the reflectivity of an ideally smooth surface given for instance by the Fresnel theory. The validity of this formula has been discussed by André (1984).

The importance of investigations of the x-ray scattering from rough surfaces becomes evident in the study of the microtopography of supersmooth surfaces for which the minimum diametrical dimensions of roughness detected by optical methods are of the same order as the probing radiation wavelength. In the x-ray range the total integrated scattering remains considerable even at a roughness of several ångströms, owing to the short wavelength of the x-ray radiation.

3. Experimental procedure

The angular and spectral dependences of reflectivity were carried out at the synchrotron radiation laboratory HASYLAB at the UHV reflectometer described by Hogrefe *et al* (1983). It allows computer-controlled independent rotations of the sample and the detector. The measurements were performed with Schottky-type diodes (Hamamatsu G1127). Since the sample can be removed from the beam, the necessary normalization was done by moving the detector into the direct beam. The corrections for changes in the incoming photon flux were made by monitoring the total electron yield from the last focusing mirror in the beam line. The monochromated radiation in the soft-x-ray region 50–1000 eV was supplied by the monochromator BUMBLE BEE whose principles and characteristic data have been described in detail elsewhere (Jark *et al* 1983, Jark and Kunz 1986). Using an appropriate configuration of the monochromator elements the spectral purity of monochromated beam can be optimized. Further improvement is achieved by the use of transmission filters (Al, Ag, In and Cu). The spectral purity in the energy range used was above 99%. The energy resolution is about 1/200; the accuracy of the energy scale is better than 0.1%.

The angular distribution of radiation scattered by the BN_{hex} surface was measured in a reflectometer set-up on the SA23 beam line of the SuperACO storage ring of the LURE at Orsay. The synchrotron radiation was monochromated by means of a toroidal grating monochromator, giving a resolution of better than 1 eV at 200 eV. The radiation impinging on the sample mirror is largely s polarized. The radiation is directly detected with a 'channeltron'. The angular resolution is about 0.15°.

4. Results and discussion

4.1. Specular reflection from the Si–SiO_2 structure

The Si–SiO_2 system with different dioxide thicknesses was investigated using s-polarized synchrotron radiation. The samples were prepared by a dry oxidation method in order to eliminate as much as possible the influence of the technological treatment on the atomic structure. The surfaces of all the samples are formed in the process of spontaneous growth of dioxide on the silicon plate. Reflection spectra $R(E)$ for grazing incidence angles of 4,

6, 10 and 15° as well as reflectivity angular dependences $R(\theta)$ were measured in the energy range 40–850 eV including the Si $L_{2,3}$ and O K absorption edges. Figures 2(a) and 2(b) show the reflection spectra near the Si $L_{2,3}$ and O K absorption edges, respectively, for a grazing angle of 4°. Analysis of the Si 2p reflection fine structure indicates that the reflection spectrum for the 120 nm sample is in good agreement with the reflection spectrum for bulk amorphous SiO_2 (Filatova *et al* 1985). The reflection spectra for the 10 nm sample display a superposition of features belonging to both the SiO_2 and the Si crystal (Vinogradov *et al* 1982). The reflection spectra for the 2.5 nm sample are mainly due to the silicon structure with a probable weak contribution of SiO_x (Filatova *et al* 1985). The comparison with the O K region confirms that the atomic structure of the surface layer of the 2.5 nm sample is characterized by an atomic composition distinguishable from SiO_2. The maxima a and b in the 120 nm sample are caused purely by interference. We obtained angular dependences of the reflection coefficient for several points in the spectral range 100–750 eV for glancing angles between 0 and 60° (figure 3). Using the angular dependences for the 120 nm sample, the real and imaginary parts of the dielectric constant were calculated for SiO_2. In this case the SiO_2 layer is thick enough for radiation almost not to penetrate through it. Only a weak interference pattern was observed at large grazing angles. Neglecting these fluctuations we can use a simple Fresnel formula for fitting. The results are presented in table 1.

The angular dependences for the 10 nm sample revealed strong interference effects. Theoretically, all five parameters could be fitted from experimental curves: two complex values of the dielectric constant and the SiO_2 layer thickness d. However, fitting appeared to be very unstable in this case. We used the value of the dielectric constant for SiO_2 determined above and fitted only the dielectric constant for the Si substrate, and the thickness d. Fresnel reflections from two interfaces were taken into account: vacuum–SiO_2 and SiO_2–Si. An example of fitting is illustrated in figure 4. The SiO_2 layer thickness d was found to be 10.7 ± 0.3 nm. The calculations were carried out very carefully because the values of the dielectric constants of Si and SiO_2 are close. The precision of the results differs very much from point to point depending on the relative values of the dielectric constants for the layer and the substrate. Also, a reliable value of δ cannot be obtained where $\delta \simeq 0$ (the shape of the angular curve is almost insensitive to δ in this case). The values of δ and β for the substrate are not monotonic in the vicinity of the O K threshold (550 eV; see table 1). Obviously, this should not be the case if the substrate were pure silicon. So, we can conclude that there is some kind of penetration of oxygen beyond the substrate–layer interface. This may be a SiO_x interlayer of unknown composition and thickness. Turning now back to the interference pattern of the 120 nm sample and knowing the dielectric constant of the substrate, we can estimate precisely the layer thickness d. It was found to be 121 ± 2 nm. Some small discrepancies between the experimental and fitted curves can be attributed to surface roughness. The value of the mean roughness height σ was also fitted in some cases using the approximation given by the Debye–Waller formula. It was always found that $\sigma < 1$ nm.

4.2. Specular reflection from BN_{hex}

The anisotropy of chemical bondings via sp^2 hybridization between B and N atoms within and perpendicular to the layers of hexagonal BN_{hex} crystals, i.e. perpendicular (or parallel) to the optical axis C, leads to strong anisotropy in the interaction of BN_{hex} with polarized radiation. Absorption must originate from transitions from B K (N K) to σ states in the case when the electric field E is perpendicular to C and to π states in the case when the electric field E is parallel to C.

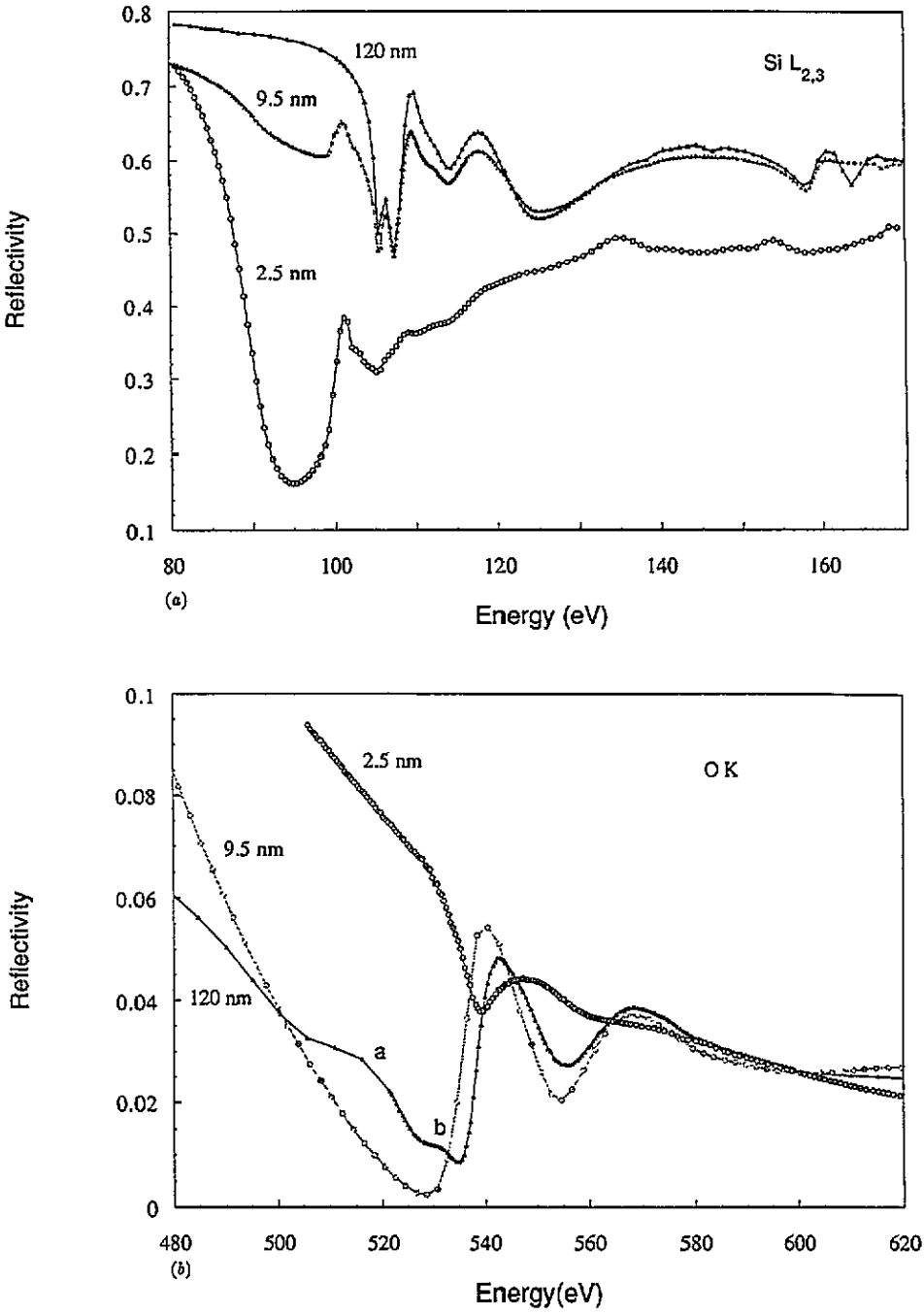

Figure 2. Reflection spectra of the Si–SiO_2 layer system for different thicknesses of the dioxide layer (2.5, 9.5 and 120 nm): (a) near the Si $L_{2,3}$ edge; (b) near the O K edge.

By turning the crystal and using s-polarized radiation, one can change the contributions of different transitions to the B K or N K absorption spectra. The reflection spectra from two

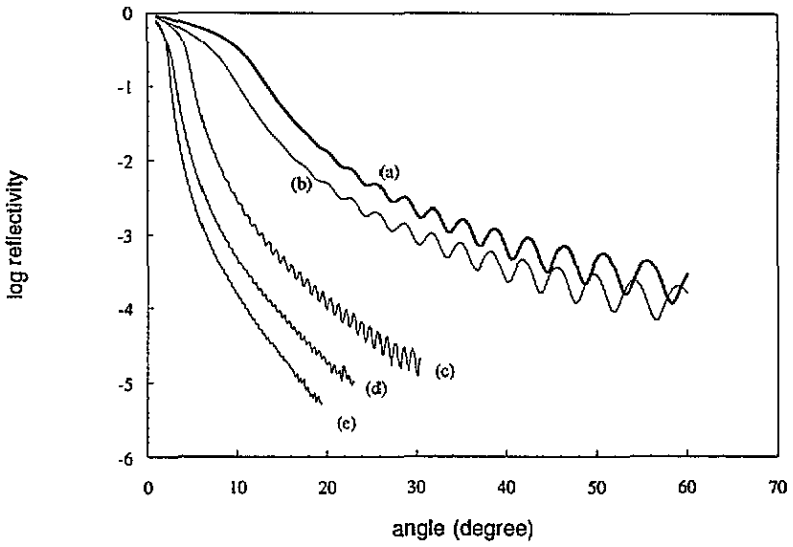

Figure 3. Reflectivity versus the glancing angle of the Si–SiO_2 layer system with a dioxide layer thickness equal to 120 nm for different x-ray energies E: curve (a) $E = 99$ eV; curve (b), $E = 105$ eV; curve (c), $E = 350$ eV; curve (d), $E = 550$ eV; curve (e), $E = 750$ eV.

Table 1. Values of the unit decrement δ of the real part and of the imaginary part β of the dielectric constants for silicon and silicon dioxide at various x-ray energies obtained from our reflectometry measurements.

	Energy (eV)	Si		SiO_2	
		$\delta(\times 10^{-3})$	$\beta(\times 10^{-3})$	$\delta(\times 10^{-3})$	$\beta(\times 10^{-3})$
1	99.00	-19 ± 4	8 ± 4	39.9 ± 0.4	17.5 ± 0.6
2	105.00	-9 ± 3	21 ± 3	23.4 ± 0.3	15.0 ± 0.6
3	125.00	2 ± 4	41 ± 5	22.2 ± 0.3	24 ± 1
4	350.00	6.9 ± 0.1	3.82 ± 0.04	6.23 ± 0.06	1.69 ± 0.06
5	500.00	3.78 ± 0.03	1.06 ± 0.01	2.73 ± 0.02	0.48 ± 0.02
6	540.00	2.25 ± 0.08	0.67 ± 0.06	2.13 ± 0.03	2.4 ± 0.1
7	550.00	2.99 ± 0.08	0.85 ± 0.05	2.50 ± 0.03	1.10 ± 0.04
8	620.00	2.38 ± 0.02	0.49 ± 0.01	2.23 ± 0.02	0.80 ± 0.03
9	750.00	1.65 ± 0.01	0.27 ± 0.01	1.65 ± 0.02	0.39 ± 0.02

surfaces cut parallel and perpendicular to the C axis of the crystal in the region 40–859 eV, i.e. including the B K and N K absorption edges, were obtained for different glancing angles. Figure 5 shows the reflection fine structure near the B K and N K absorption edges. The B K reflection spectra of $BN_{parallel}$ and BN_{perp} have similar numbers of features and similar energy dependences. At the same time, a strong intensity dependence on the crystal orientation obviously exists for peaks A and B in the reflection spectra at 8 and 10°, whereas this effect in the reflection spectra at 4° is rather weak. According to Filatova and Blagoveschenskaya (1991), the technological treatment of the sample surface produces a mechanically distorted surface layer. The existence of such a disordered layer makes the situation closer to polycrystalline and therefore weakens the effect of sample orientation. Since an increase in the glancing angle leads to a greater probing depth, more perfect layers participate in the formation of the reflected radiation beam. The intensity of peak A

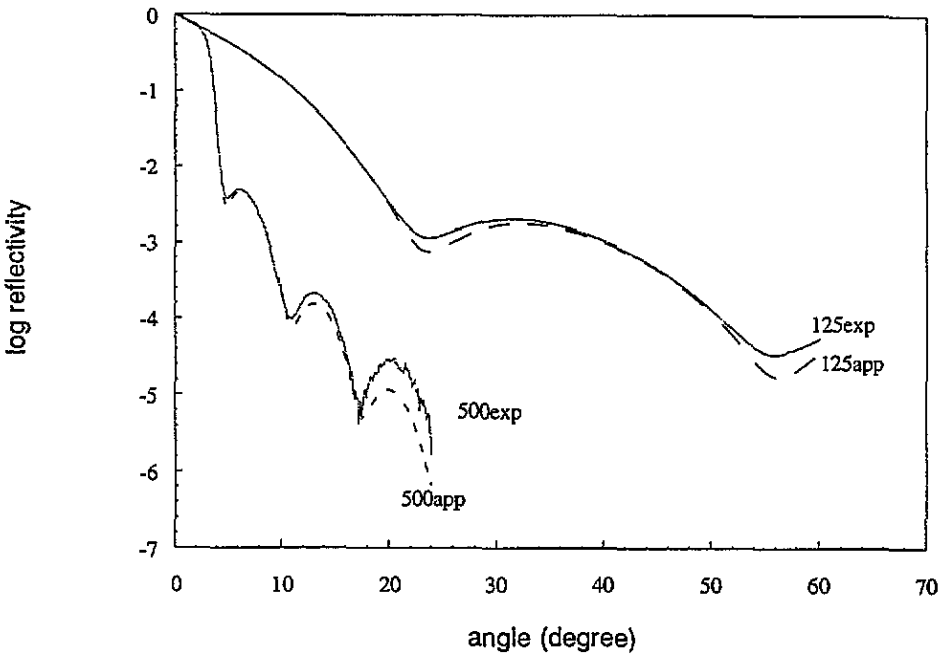

Figure 4. Experimental (——) and fitted (- - - -) reflectivity versus the glancing angle of the $Si–SiO_2$ layer system with a dioxide layer thickness close to 10 nm for different x-ray energies of 500 and 125 eV.

is considerably higher for $BN_{parallel}$ than for BN_{perp}. Quite different behaviour occurs for the intensity of peak B (higher intensity in the case of BN_{perp}). An analogous orientation dependence of B K reflection spectra was obtained by Filatova and Blagoveschenskaya (1993) using the unpolarized radiation of an x-ray tube but the effect is more obvious at small glancing angles when observed with linearly polarized synchrotron radiation.

Figure 6 shows the B K and N K absorption spectra for both crystal orientations calculated from the reflection spectra at 4° using the Kramers–Kronig relationship and combined in a common scale by means of XPS data (Hainrim 1970). Although application of the Kramers–Kronig relationship in this case does not guarantee accuracy of the absolute value of the dielectric constant, it describes the shape of the spectra correctly. A comparison of the B K and N K absorption spectra (figure 6) shows that the N K spectra demonstrate features similar to the B K spectra, which means that both boron and nitrogen 2p states participate in the formation of π- and σ-like molecular orbitals of BN_{hex}. According to theoretical calculations (Nakhmanson and Smirnov 1972, Robertson 1984), peaks a and a′ correspond to transitions to the π_1 and π_2 states, and maxima b and c to the σ_1 and σ_2 states. The orientation dependences support this conclusion. At the same time the relative intensities of peaks a and a′ in the B K and N K spectra reveal strong differences. This reflects the much larger contribution of B p_π states to the π_1 resonance than to the π_2 resonance, while the contribution of N p_π states to the π_2 resonance is on the contrary larger. The detailed explanation of all features of the B K and N K absorption spectra can be given on the quasi-atomic approach, but it is beyond the scope of this paper.

4.3. Scattering from BN_{hex} rough surface

To obtain information on the crystal surface roughness, the angular distributions of the diffusely scattered radiation (scattering indicatrices) were obtained for different radiation energies and angles, and two boron nitride crystal samples with different types of surface. The sample denoted BN and the sample denoted BN* have not undergone the same surface treatment. Thinner abrasive powder was used to polish the BN* sample. Only the surface perpendicular to the C crystal axis was studied. Let us consider for example the scattering indicatrices for $E = 150$ eV at different glancing angles given for the BN* and BN samples in figures 7(a) and 7(b), respectively. All measurements show a large amount of radiation diffusely scattered by the surface. At first sight it seems that some of the scattered radiation remains in the vicinity of the specularly reflected radiation since the width of the main peak is larger than the width of the specular component (0.2°), while another part of the scattered radiation moves with respect to the specular direction when the glancing angle is changed. In terms of surface roughness statistics, this should mean that the first type of roughness having a large autocorrelation length gives rise to scattering along the specular direction while the second type of roughness having a smaller autocorrelation length is responsible for the other scattered radiation. The behaviour of the scattering attributed to the short autocorrelation length is very similar to the mechanism of the phenomenon known as the Yoneda effect, explained in detail by different workers (Croce *et al* 1972, Vinogradov 1988, Alehyane *et al* 1989, Filatova and Blagoveschenskaya 1992). The main features of the phenomenon can be summarized as follows. When the autocorrelation length is sufficiently small, the scattering angular distribution presents a peak in the angular distribution at an angle located near the critical angle, limiting the region of total reflection. More precisely, this structure results from the peaked profile of the quantity $\cos^2\theta_2 Q(\theta_1, \theta_2, \theta_3, \varepsilon)$ versus the scattering angle θ_2 (see equation (6)) near the critical angle; a peak called the Yoneda (1963) peak is actually observable provided that the PSDF presents a non-vanishing value in the vicinity of this angle, which requires a sufficiently short correlation length and a corresponding mean value σ which is not too small.

Although the phenomena are qualitatively fairly well understood, an estimation of the statistical parameters is rather complicated for several reasons.

(1) Only perturbation methods assuming that the mean height of the roughness is small with respect to the wavelength are available in analytical forms, but in the x-ray region this assumption is generally not satisfied.

(2) The number of parameters to fit is generally very large; different types of surface roughness with unknown autocorrelation functions may be involved in the problem; volume scattering may also be implicated and the in-depth spatial distribution of scatterers is generally unknown.

(3) Basically, this kind of problem belongs to the class of inverse problems which present important theoretical difficulties: non-uniqueness, ill-conditioned problem, etc.

Nevertheless, one can attempt to perform some quantitative estimates using the following considerations. It was shown in particular situations that even in the case where the perturbation method diverges, the shape of the angular distribution remains physically acceptable (Sammar and André 1991). Estimation of the autocorrelation radius by a fitting procedure using a perturbation model has given values in fair agreement with data obtained by other methods (Alehyane *et al* 1989).

In our numerical simulations we assume that the ACF is a Gaussian isotropic function and we proceed as follows. The scattering angle for which the scattering angular distribution corresponding to the short autocorrelation component of the surface roughness peaks,

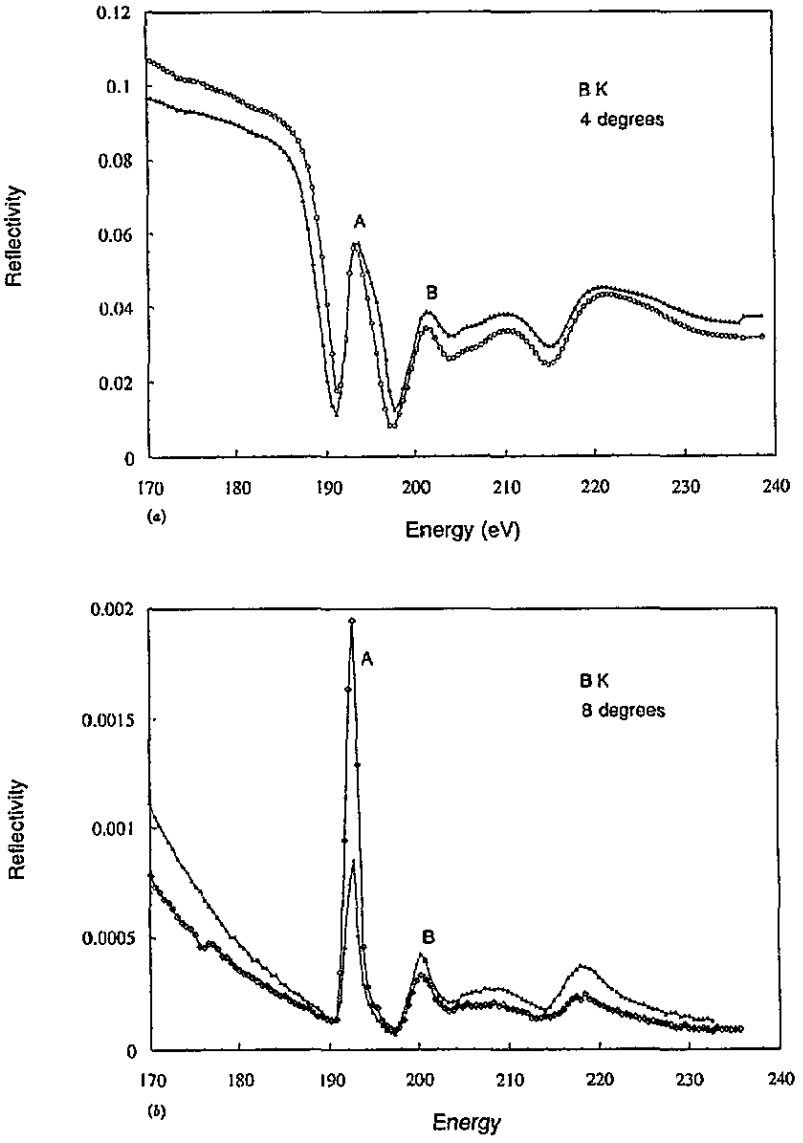

Figure 5. Reflection spectra of the boron nitride hexagonal crystal near the B K edge and the N K edge depending on the orientation of the crystal axis C with respect to the electric field E (·····: C and E perpendicular; ——, C and E parallel) for glancing angles θ: (a) B K edge, $\theta = 4°$; (b) B K edge, $\theta = 8°$; (c) B K edge, $\theta = 10°$; (d) N K edge, $\theta = 4°$.

corresponds to the critical angle $\sqrt{\delta}$ and gives $\mathrm{Re}(\varepsilon)$. The imaginary part $\beta = \mathrm{Im}(\varepsilon)$ is approximately estimated by the shape of the peak reflectivity curve versus the glancing angle; in fact the shape of this curve depends on the ratio β/δ (André *et al* 1984). From $\sqrt{\delta}$ and β, one deduces ε. Assuming a Gaussian shape for the ACF and taking into account the value of ε previously determined, one tries to obtain a value of the short autocorrelation radius T_s using equations (6) and (7) by fitting the experimental indicatrices, especially in the tails of the curves. We estimate the value of the short autocorrelation radius to be $T_s = 800 \pm 200$ nm for both samples.

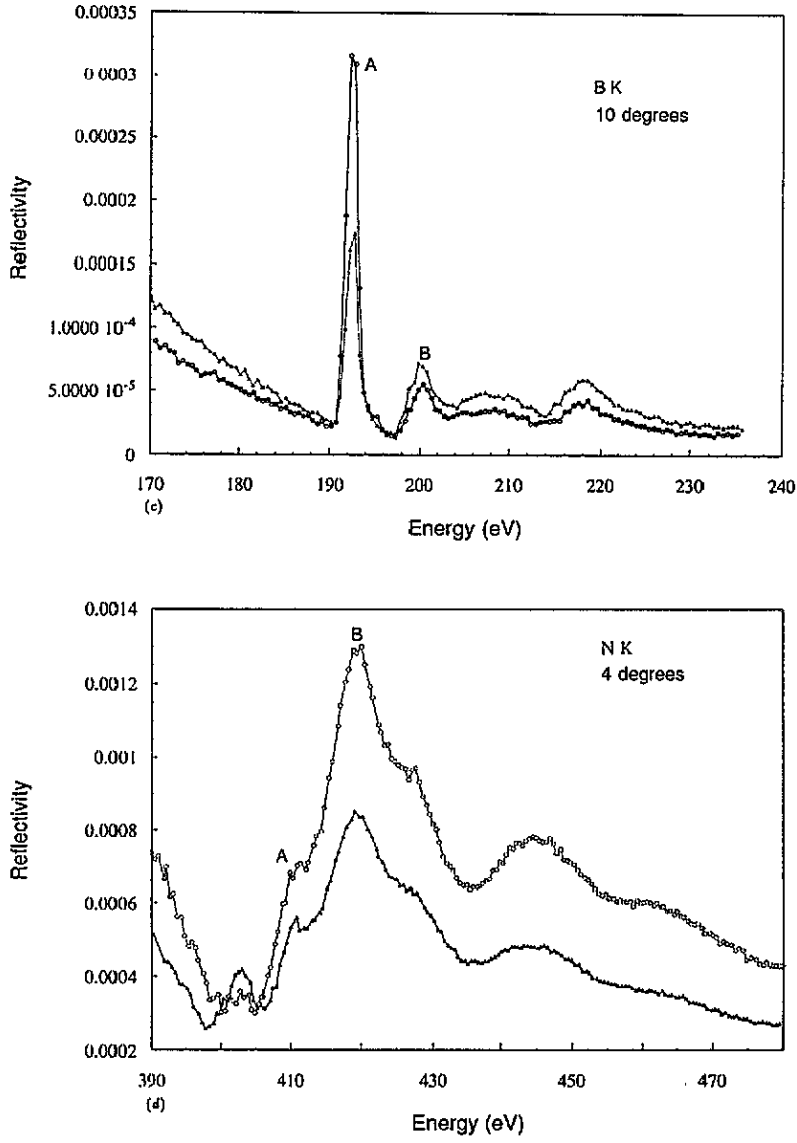

Figure 5. (Continued)

The large autocorrelation radius cannot be easily estimated because of the presence of the specular component. The average height σ of the microroughness is about 12 nm for both samples. To estimate the average height σ of the microroughness, we have assumed that the peak reflectivity is attenuated according to a Debye–Waller law. The validity of this assumption is very questionable and has been discussed previously (André 1984). Moreover the peak reflectivity is difficult to estimate from measurements since the specular reflection is embedded within diffuse scattered radiation coming from the large autocorrelation roughness. In fact, σ is rather a quality parameter which lumps the various effects of the surface microroughness on the specular reflectivity. Rigorously one should define a specific σ for the short autocorrelation component of the surface roughness and

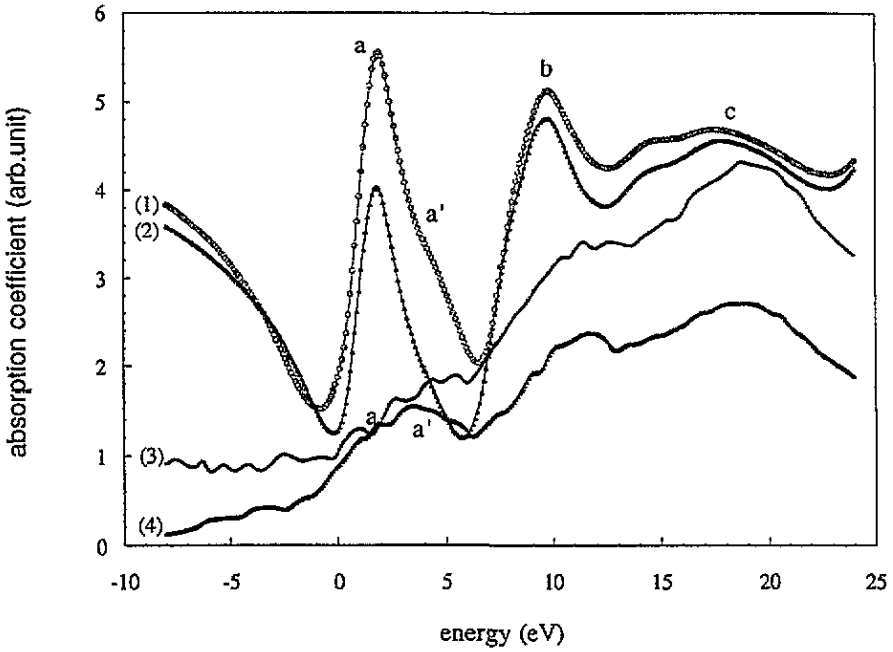

Figure 6. B K and N K absorption spectra of the boron nitride hexagonal crystal for both orientations calculated from the reflection spectra at 4° using the Kramers–Kronig relationship and combined in a common scale: curve (1), B K edge parallel configuration; curve (2), B K edge perpendicular configuration; curve (3), N K edge perpendicular configuration; curve (4), N K edge parallel configuration.

another for the large autocorrelation component. The two samples BN* and BN differ essentially in their relative proportions of the large and short correlation components which cannot be easily evaluated.

5. Conclusions

We have obtained at different energies the variation in the reflectivity of the Si–SiO_2 layer system with the glancing angle for different dioxide thicknesses and shown that it is possible to estimate the thickness of the oxide layer with a relative accuracy better than 3% by means of the Fresnel theory of specular reflection. The low divergence and high flux of the synchrotron radiation is very useful for this kind of reflectometry experiment since it allows very good collimation of the incident beam and consequently a well defined glancing angle. The dielectric constants for silicon and silicon dioxide have been calculated from reflectivity angular dependences on a wide spectral range by virtue of the broad spectrum available with the synchrotron radiation. We have recorded the x-ray reflection spectra near the K absorption edges of a BN_{hex} crystal and shown the advantages of the linear polarization of the synchrotron radiation for studying the electronic structure of an anisotropic crystal. The angular distribution of the radiation diffusely scattered by the rough surface of BN_{hex} crystals was investigated. The low divergence of the incident beam allowed by the synchrotron radiation is very useful for this kind of measurement since it reduces the effect of convolution. The statistical properties of the roughness were estimated on the

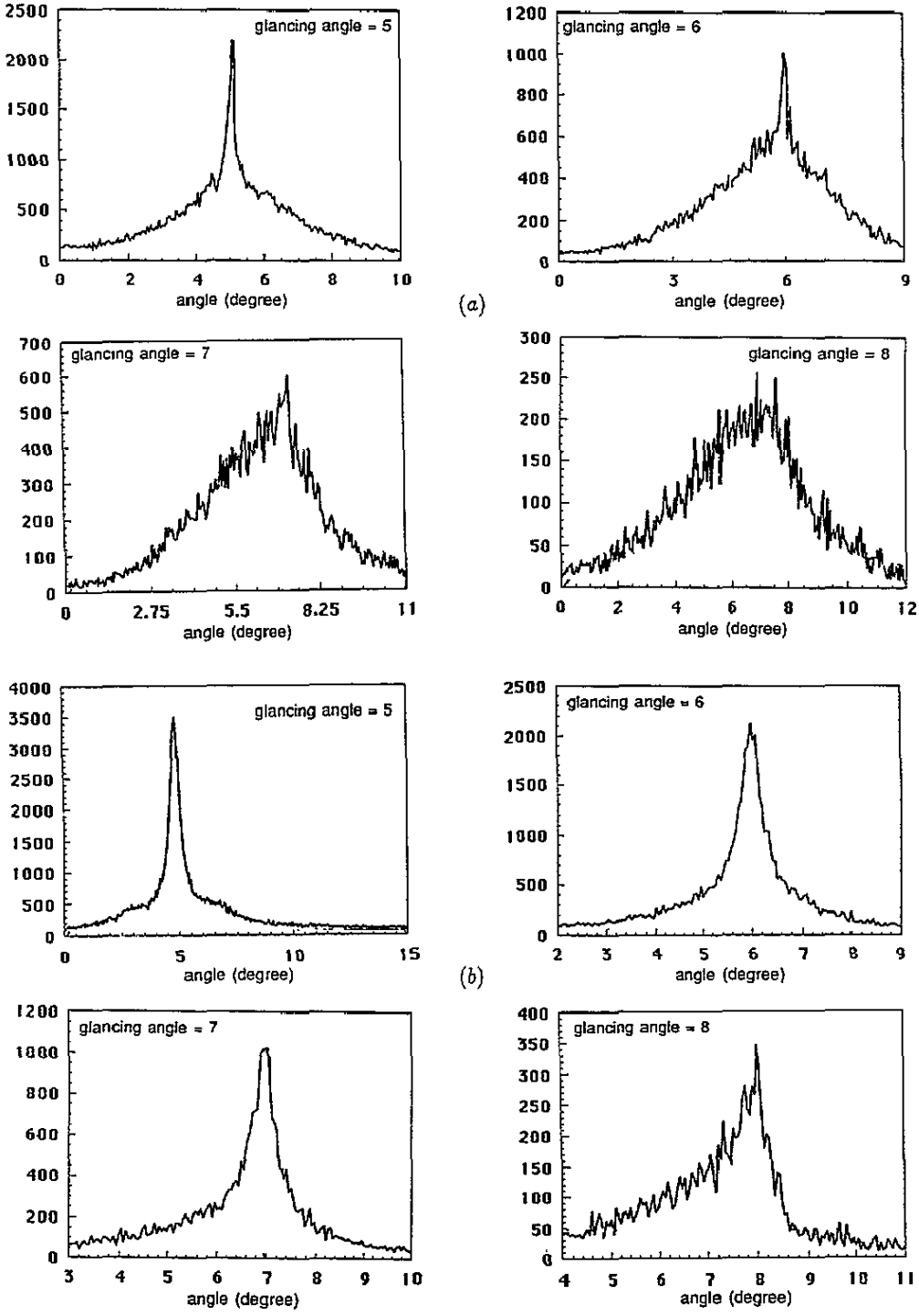

Figure 7. Angular distribution of the radiation diffusely scattered by the surface roughness for two different boron nitride crystal samples for different glancing angles: (a) BN* sample; (b) BN sample. The samples differ in the nature of their surface treatments. The energy of the x-ray photon is 150 eV.

basis of a perturbation theory. The results obtained here demonstrate that soft-x-ray total reflection spectroscopy is a very efficient non-destructive method of material diagnostics owing to the high sensitivity to the chemical composition of substance, atomic arrangement and presence of interfaces. The use of synchrotron radiation makes it possible to realize the capabilities of soft-x-ray reflection spectroscopy and roughness scattering measurements to the greatest extent.

References

Alehyane N, Arbaoui M, Barchewitz R, André J-M, Christensen F, Hornstrup A, Palmari J, Rasigni M, Rivoira R and Rasigni G 1989 *Appl. Opt.* **28** 1763

André J-M 1984 *Opt. Commun.* **52** 87

André J-M, Barchewitz R, Maquet A and Marmoret R 1984 *Phys. Rev.* B **30** 6576

André J-M, Maquet A and Barchewitz R 1982 *Phys. Rev.* B **25** 5671

Croce P, Névot L and Pardo B 1972 *C. R. Acad. Sci., Paris* **274** 855

Elson J M 1984 *Phys. Rev.* B **30** 5460

Filatova E O and Blagoveschenskaya T A 1991 *Pis. Zh. Tekh. Fiz.* **17** 14

—— 1992 *J. X-ray Sci. Tech.* **3** 204

—— 1993 *J. X-ray Sci. Tech.* **4** 1

Filatova E O, Vinogradov A S, Zimkina T M and Sorokin I A 1985 *Sov. Phys.–Solid State* **27** 603

Greaves G N, Pizzini S, Barrett N T, Roberts K J and Kalbitzer S 1990 *Proc. 6th Int. Conf. on X-ray Absorption in Fine Structure*; (*Daresbury Laboratory, Warrington, UK, Report* DL/SCI/P722E)

Hainrim K 1970 *Phys. Scr.* **1** 277

Hogrefe H, Giesenberg D, Haelbich R-P and Kunz C 1983 *Nucl. Instrum. Methods* **208** 415

Hogrefe H and Kunz C 1987 *Appl. Opt.* **26** 2851

Jark W, Haelbich R-P, Hogrefe H and Kunz C 1983 *Nucl. Instrum. Methods* **208** 315

Jark W and Kunz C 1986 *Nucl. Instrum. Methods* A **246** 320

Maradudin A A and Mills D L 1975 *Phys. Rev.* B **11** 1392

Martens G and Rabe P 1980 *Phys. Status Solidi* a **58** 415

Nakhmanson M S and Smirnov V 1972 *Sov. Phys.–Solid State* **13** 2763

Noll R J and Glenn P 1982 *Appl. Opt.* **21** 1824

Parratt L G 1954 *Phys. Rev.* **95** 359

Robertson J 1984 *Phys. Rev.* B **29** 4

Sammar A and André J-M 1991 *Opt. Commun.* **86** 245

Vinogradov A V 1988 *Sov. Phys.–JETP* **67** 389

Vinogradov A S, Filatova E O and Zimkina T M 1982 *Sov. Phys.–Solid State* **24** 979

Yoneda Y 1963 *Phys. Rev.* **131** 2010